

# Short-Range Structural Transformations in Water at High Pressures

Ramil M. Khusnutdinoff<sup>a</sup> Anatolii V. Mokshin<sup>a</sup>

<sup>a</sup>*Department of Physics, Kazan (Volga region) Federal University, Kremlevskaya Street 18, 420008 Kazan, Russia*

---

## Abstract

We report results of molecular dynamics simulations of liquid water at the temperature  $T = 277$  K for a range of high pressure. One aim of the study was to test the model Amoeba potential for description of equilibrium structural properties and dynamical processes in liquid water. The comparison our numerical results with the Amoeba and TIP5P potentials, our results of *ab initio* molecular dynamics simulations and the experimental data reveals that the Amoeba potential reproduces correctly structural properties of the liquid water. Other aim of our work was related with investigation of the pressure induced structural transformations and their influence on the microscopic collective dynamics. We have found that the structural anomaly at the pressure  $p_c \approx 2000$  Atm is related with the changes of the local, short-range order in liquid water within first two coordination shells. This anomaly specifies mainly by deformation of the hydrogen-bond network. We also discuss in detail the anomalous behavior of sound propagation in liquid water at high pressures and compare numerical results with the experimental data.

*Key words:* Amoeba water model, molecular dynamics, structural anomaly, dynamic structure factor, hydrogen-bond network

*PACS:* 61.20.Ja, 61.25.Em, 67.25.dt, 68.35.Rh

---

## 1 Introduction

Water is one of the most widespread liquids in wildlife and has a great number chemical and technological applications [1]. Although a particular water molecule has a simple chemical structure, a water system is considered as a

---

*Email address:* khrm@mail.ru (Ramil M. Khusnutdinoff).

complex fluid because of its anomalous behavior in thermodynamical, structural and transport properties [2]. It dilates with solidification, and the density has a maximum at the pressure 1.0 Atm and the temperature 277 K [3]. Additionally, there is a minimum in the isothermal compressibility at 319 K and a clear minimum in the isobaric heat capacity at 308 K. These anomalies are linked with the microscopic structure of liquid water [4], which can be regarded as a *transient gel* – a highly associated liquid with strongly directional hydrogen bonds [5,6].

An active study of the different characteristics and properties of water system is provided by the development of the numerical methods of the computer simulations. So, the first study of the water “structure” was performed by Barker and Watts within Monte-Carlo method [7]. They have computed the energy, heat capacity and radial distribution function for water system at the temperature 298 K and have compared the obtained results with the experimental data. The considered system was very small, 64 molecules interacted via the Rowlinson potential [8]. In the next study performed by Rahman and Stillinger [9] the water system was simulated through 216 rigid molecules interacted by means of the pair-additive effective potential. The authors have investigated in detail the structural, transport and dynamic properties of liquid water at the temperature 307.3 K. The molecular dynamics simulations in the low temperature thermodynamic phase range were performed by Ref. [10]. Here, the “*second critical point*” at the temperature  $T = 223$  K and pressure  $p = 1000$  Atm was found. Below this second critical point, the liquid phase separates into two distinct phases – a *low-density liquid* and a *high-density liquid*. It is necessary to note that to study the water system a great number of the model potentials for intramolecular and intermolecular interactions were suggested (see, for example, review [11]). Here, the first model of the liquid water was proposed in 1933 by Bernal and Fowler [12]: an ice-like disordered tetrahedral structure arising from the electrostatic interactions between close neighbors.

The special role in the understanding of the microdynamic features of the water have the methods of *ab-initio* simulations based on the density functional theory. So, one of the first works, where the Car-Parrinello method was applied to study dynamic properties in water, was done by Laasonen *et al.* [13]. They also found that the local density approximation gives realistic results for the intramolecular properties without gradient corrections, but it fails to give a correct description of the intermolecular interactions and the binding properties. Later, the numerous *ab-initio* simulations for water system have been done [14,15,16,17,18].

Recently, a large amount of the works were intended for the investigation of water structural, transport, mechanical properties at the different externally applied conditions [19,20,21,22,23]. For example, the processes of the disso-

ciation of the water molecules at the pressures 14.5 GPa and 26.8 GPa were investigated in Ref. [24] by means of *ab-initio* molecular dynamics simulations. Molecular dynamics simulations of water at the negative pressures were carried out with two model potentials of interparticle interaction: the extended simple point charge (SPC/E) and the Mahoney-Jorgensen transferable intermolecular potential with five points (TIP5P). The equilibrium phase diagram was constructed in Ref. [25] for a wide range of temperature and pressure by means of Monte-Carlo simulations within two model potentials, TIP4P and SPC/E. Then, the correlation between structural and dynamical anomalies in supercooled water was studied [26] on the basis of the SPC/E potential.

Some of works were pointed mainly towards the study of structural and dynamical properties related with the anomalous features of liquid water [27,28,29,30,31,32,33,34,35]. The concepts of low-density water (LDW) and high-density water (HDW) were suggested in Ref. [27] on the basis of the experimental data of neutron diffraction, which detected clear the structural transformations in liquid water [28]. Further, the structural transition from LDW to HDW as well as the anomalies related with these structural transformations were extensively considered [29,30,31,32,33,34]. An comprehensive overview of the properties of supercooled and glassy water, the transition between low-density amorphous (LDA) ice and high-density amorphous (HDA) ice were presented in Ref. [35]. Nevertheless, in spite of the numerous studies, the question about the impact of structural transition from LDW to HDW on the dynamical properties and anomalies of water is still open [3].

In this work we perform the numerical study of the structural transformations in water, which are appeared at the fixed temperature  $T = 277$  K with the change of the externally applied pressure  $p = 1.0 \div 10\,000$  Atm. In addition, the influence of the structural rearrangements on the dynamical properties in liquid water is also considered. Other aim of the work is related with the test of the Amoeba potential [36,37,38] to describe the structural and dynamical features of water.

The paper is organized in the following way. In the next section, we describe the details of the molecular dynamics simulations of liquid water on the basis of the Amoeba model potential. A detailed analysis of the pressure dependence of the static properties and the structure anomalies are then reported. Then, the features in the dynamic and dispersion of sound velocity are reported and compared with the experimental data on inelastic X-rays scattering. The role of the hydrogen-bond network in the structural transformation is discussed. And, finally, we conclude with a short summary.

## 2 Computational Details

Equilibrium classical molecular dynamics (MD) simulations of water at the constant temperature  $T = 277$  K and the different pressures were carried out with the TINKER molecular modeling package [36]. We use the Amoeba (Atomic Multipole Optimized Energetics for Biomolecular Applications) water model, which was recently suggested by Ren and Ponder [37,38]. Our computations were performed for 4000 water molecules interacted within a cubic box, where the periodic boundary conditions were imposed in all directions. The Ewald summation was used to handle the electrostatic interactions as well as an atom-based switching window of the size  $12 \text{ \AA}$  was applied to cut off the van der Waals interactions. The equations of motion were integrated via a modified Beeman algorithm [39] with the time step  $\Delta\tau = 1.0$  fs. The MD calculations were performed in the isothermal-isobaric ensemble at the temperature  $T = 277$  K and the pressure  $p = 1.0, 1000, 2000, 3750, 5000, 7797$  and  $10000$  Atm, where we used the Berendsen thermostat and barostat [40] to enforce the constant temperature and pressure.

## 3 Results

### 3.1 Partial Radial Distribution Functions

The radial distribution function (RDF) provides directly the information about the average packing the molecules in water and can be extracted from neutron [41] and X-ray scattering data [42]. On the other hand, this term in an extended form can be calculated on the basis of MD simulation data [43], namely

$$g_{\alpha,\beta}(r) = \frac{L^3}{N_\alpha N_\beta} \left\langle \sum_{j=1}^{N_\alpha} \frac{n_{j\beta}(r)}{4\pi r^2 \Delta r} \right\rangle, \quad (1)$$

where  $g_{\alpha,\beta}(r)$  is the probability to find an atom in the range  $[r, r + \Delta r]$  and  $L$  is the length of the box edge. The indexes  $\alpha$  and  $\beta$  define the type of the atom,  $\alpha, \beta \in \{O, H\}$ , whereas  $N_\alpha$  and  $N_\beta$  are the particle numbers of the type  $\alpha$  and  $\beta$ , respectively. The quantity  $n_{j\beta}(r)$  specifies the number of  $\beta$ -atoms located at a distance  $r$  from a  $j$ th atom within a spherical layer of the thickness  $\Delta r$ .

In Fig. 1, the partial RDF's of atoms  $g_{\alpha,\beta}(r)$  ( $\alpha, \beta \in \{O, H\}$ ) obtained from our simulations with the Amoeba potential at the temperature  $T = 277$  K and the pressure  $p = 1.0$  Atm are compared with the molecular dynam-

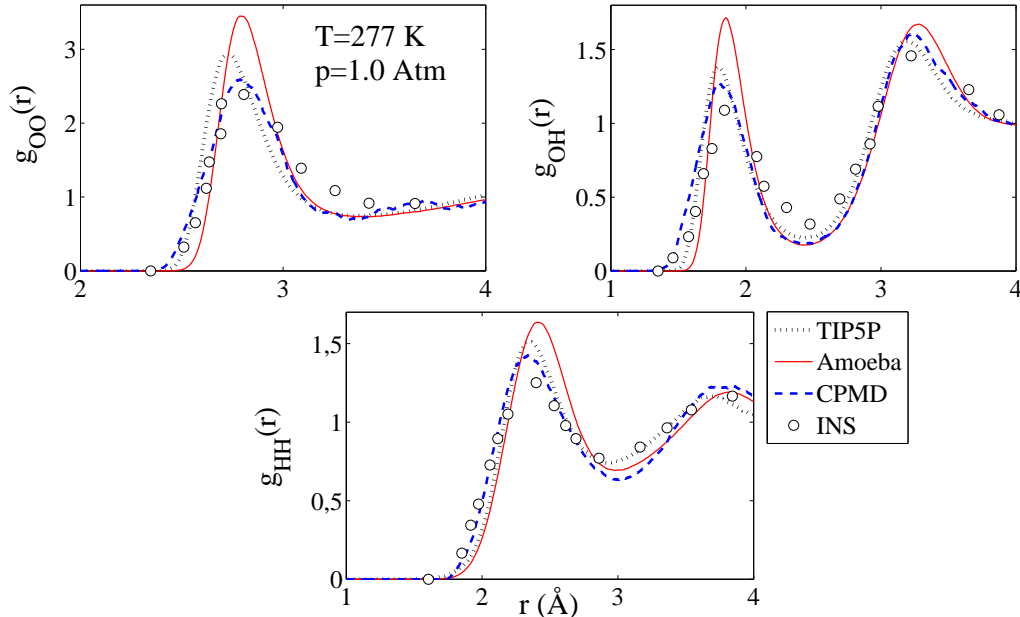


Fig. 1. (color online) Partial radial distribution functions of atoms  $g_{\alpha,\beta}(r)$  ( $\alpha, \beta \in \{O, H\}$ ) at the temperature  $T = 277$  K and the pressure  $p = 1.0$  Atm. Solid line represents the results of classical molecular dynamics simulation with the Amoeba potential; dotted line show the results of molecular dynamics simulations with the TIP5P potential; dashed line represents the results of Car-Parrinello molecular dynamics simulation for the system with 64 molecules [47]; circles are the experimental data on neutron diffraction [48].

ics simulations with the TIP5P potential, results of *ab-initio* Car-Parrinello molecular dynamics [47] and experimental data on neutron diffraction [48]. Although molecular dynamics simulations data with the Amoeba potential overestimate insignificantly the high of the first peak in partial RDF's in comparison with experimental data and results of *ab-initio* molecular dynamics simulations, they reproduce correctly the structure of liquid water at the temperature  $T = 277$  K and the pressure  $p = 1.0$  Atm. Moreover, the comparison reveals that the model TIP5P has a better agreement with experimental data and results of *ab-initio* molecular dynamics simulations.

The pressure dependence of the partial RDF for water is presented in Fig. 2. As one can see from the figure, the partial contributions of RDF for the pairs H-H and O-H remain unchanged practically at the increase of the pressure. The remarkable changes are observed in the pressure dependence of RDF for O-O pairs and indicate clear on the transition pressure  $p_{tr} \sim 2000$  Atm. It is interesting that the atomic rearrangements corresponding to the structural transformation are restricted to the second coordination sphere, where the shift of the second peak in  $g_{OO}(r)$  to the range of the high  $r$  occurs.

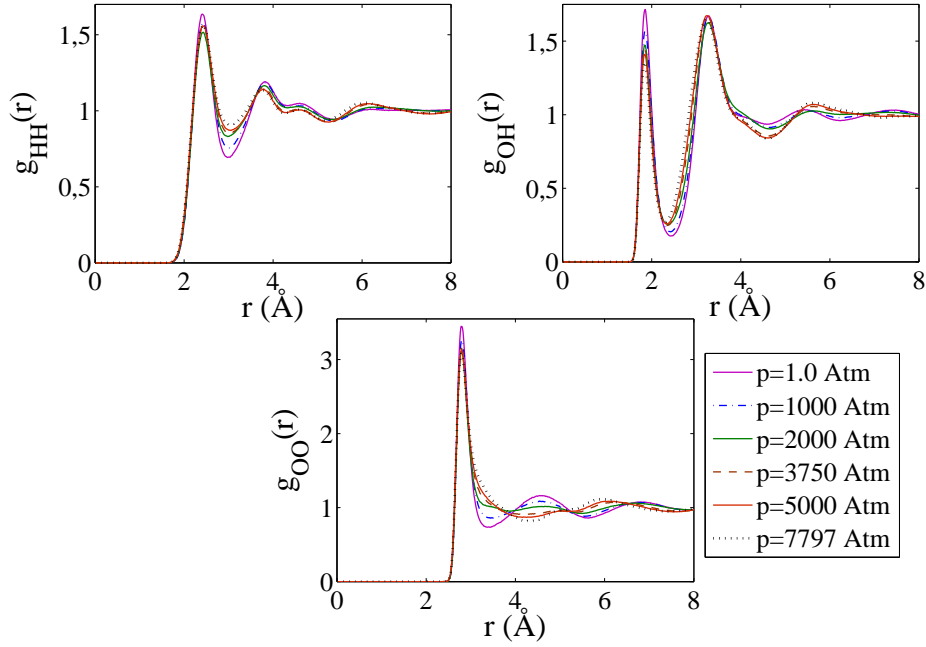


Fig. 2. (color online) Partial radial distribution functions of atoms  $g_{\alpha,\beta}(r)$  ( $\alpha, \beta \in \{O, H\}$ ) at the temperature  $T = 277$  K and the different pressures.

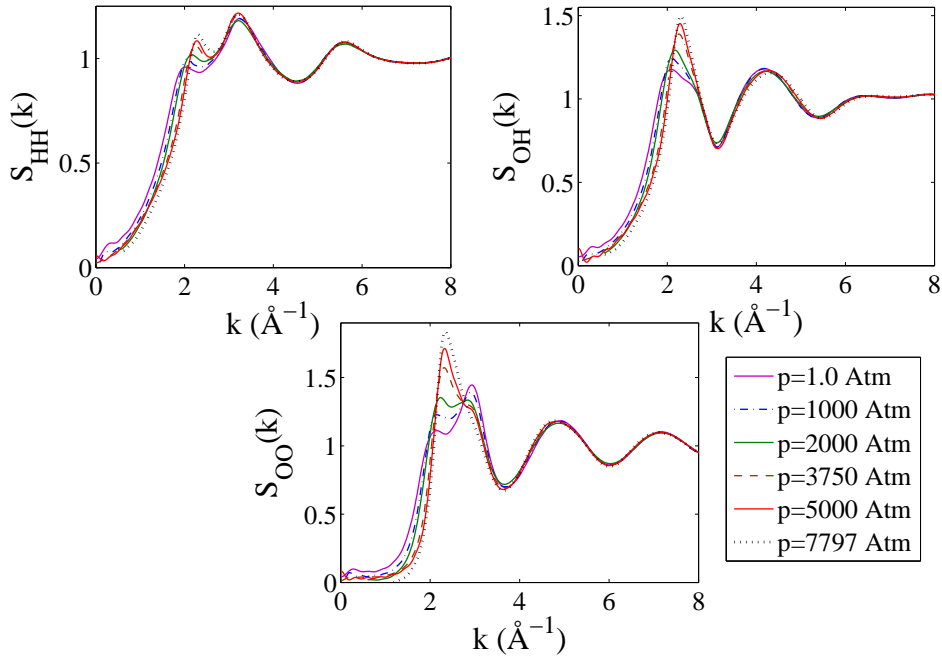


Fig. 3. (color online) Partial static structure factor  $S_{\alpha,\beta}(k)$  ( $\alpha, \beta \in \{O, H\}$ ) at the temperature  $T = 277$  K and the different pressures.

### 3.2 Partial Static Structure Factors

Other term, which is sensitive to the structural transformations, is the static structure factor,  $S(k)$ . This term is measured experimentally and is defined as [43]

$$S(k) = \frac{1}{N} \left\langle \sum_{j=1}^N e^{-i\mathbf{k}\mathbf{r}_j} \sum_{l=1}^N e^{i\mathbf{k}\mathbf{r}_l} \right\rangle. \quad (2)$$

Here,  $\mathbf{k}$  is the wave-vector and  $k = |\mathbf{k}|$ ;  $\mathbf{r}_j(t)$  defines the radius-vector of an  $j$ th atom. The partial static structure factor  $S_{\alpha,\beta}(k)$ , as an extension of  $S(k)$ , is directly related with the Fourier transform of the radial distribution function [39]:

$$S_{\alpha,\beta}(k) = 1 + 4\pi n \int_0^{\infty} r^2 \left[ g_{\alpha,\beta}(r) - 1 \right] \frac{\sin(kr)}{kr} dr, \quad (3)$$

where  $n = N/V$  is the numerical density.

The partial static structure factor  $S_{\alpha,\beta}(k)$  at various pressures for different atom pairs, H-H, O-H and O-O, is presented in Fig. 3. As can be seen, the features in the first peak of  $S_{\alpha,\beta}(k)$  become more pronounced with the increase of pressure that indicates on the rise of the short-range order. Further, the split of the first peak in  $S_{\text{OO}}(k)$  disappears with the increase of pressure that is related with the local molecular ordering in the vicinity of the first coordination shell.

### 3.3 Wendt-Abraham Parameter, Pair-Correlation Entropy and Translational Order Parameter

An additional information about the local structural features of the system can be extracted with the help of the extended Wendt-Abraham parameter

$$r_{\alpha,\beta}^{WA} = \frac{g_{\alpha,\beta}^{min}(r)}{g_{\alpha,\beta}^{max}(r)}, \quad (4)$$

where  $g_{\alpha,\beta}^{max}(r)$  and  $g_{\alpha,\beta}^{min}(r)$  represent the main maximum and the first minimum in a partial radial distribution function, respectively [49]. The thermodynamic excess entropy of a fluid is defined as the difference in entropy between

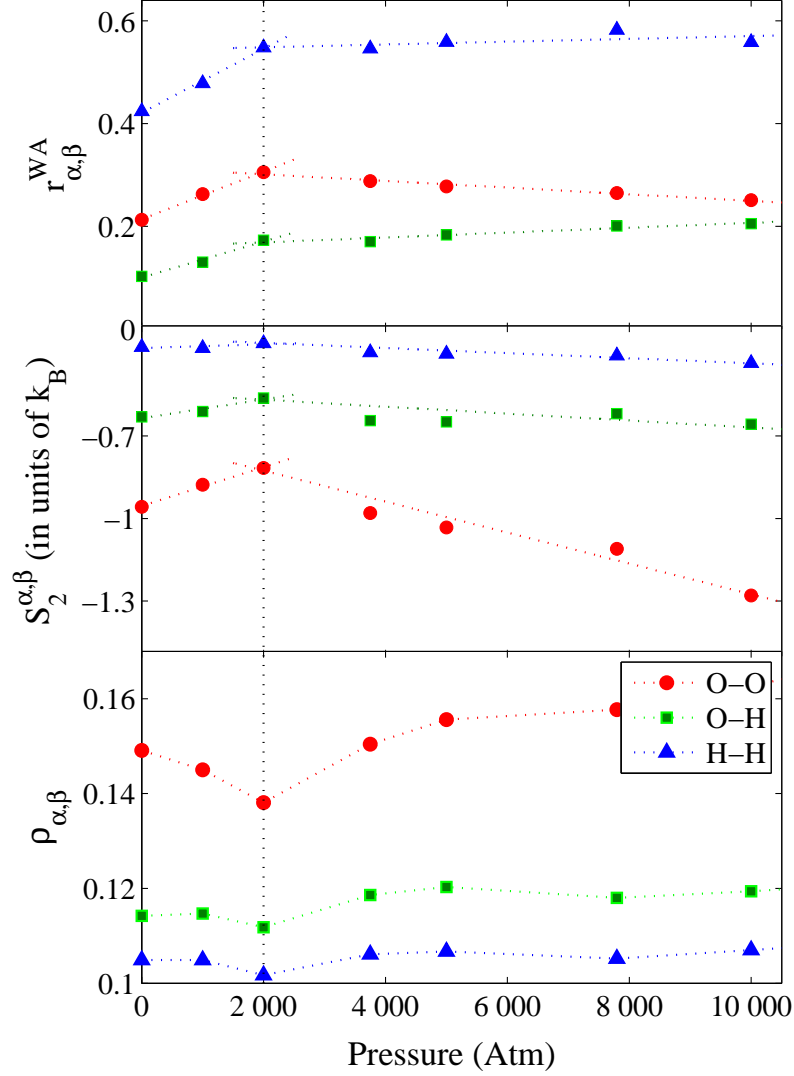


Fig. 4. (color online) Pressure dependence of the partial Wendt-Abraham parameter  $r_{\alpha,\beta}^{WA}$ , the partial pair-correlation entropy  $S_2^{\alpha,\beta}$  and the partial translational order parameter  $\rho_{\alpha,\beta}$ , where  $\alpha, \beta \in \{O, H\}$ .

the fluid and the corresponding ideal gas under identical temperature and density conditions. The total entropy of a classical fluid can be written as

$$S = S_{id} + \sum_{n=2}^N S_n, \quad (5)$$

where  $S_{id}$  is the entropy of the ideal gas reference state,  $S_n$  is the entropy contribution due to  $n$ -particle spatial correlations. Then, the excess entropy is defined as

$$S_{ex} = S - S_{id}. \quad (6)$$

The main contribution of  $S_{ex}$  for classical fluids is a pair-correlation entropy  $S_2$  (for example, in case of a monoatomic liquids this two-particle contribution to the excess entropy is 85 ÷ 95% over a fairly wide range of densities), which can be given in the extended form as

$$S_2^{\alpha,\beta} = -2\pi n \int_0^\infty \left\{ g_{\alpha,\beta}(r) \ln(g_{\alpha,\beta}(r)) - [g_{\alpha,\beta}(r) - 1] \right\} r^2 dr, \quad (7)$$

where the term  $S_2$  is measured in units of  $k_B$ .

The translational order parameter  $\rho$  is a simple and convenient measure to test the radial ordering in the studied system [50]. The separation of  $\rho$  into partial contributions can be written as the following

$$\rho_{\alpha,\beta} = \frac{1}{r_m} \int_0^{r_m} |g_{\alpha,\beta}(r) - 1| dr, \quad (8)$$

where  $r_m$  is the distance at which the structural features of the system cease to be considered. The value of  $r_m$  corresponds to a half of the edge of the simulation box. It is clear that an increase of  $\rho_{\alpha,\beta}$  indicates directly on the growth of structural radial ordering, whereas the increase of  $r_{\alpha,\beta}^{WA}$  and  $S_2^{\alpha,\beta}$  manifests the processes of structural disordering in the system.

Figure 4 illustrates the pressure dependence of the partial Wendt-Abraham parameter  $r_{\alpha,\beta}^{WA}$ , the partial pair-correlation entropy  $S_2^{\alpha,\beta}$  and the partial translational order parameter  $\rho_{\alpha,\beta}$  at the fixed temperature  $T = 277$  K. The decrease of  $r^{WA}$  indicates on the increase of the two-particle chain clusters in the system, which appear, e.g., due to the system densification and precedes the transition of the system into a solid (crystalline or amorphous) phase. As can be seen from the figure, all parameters discover the change in the pressure dependence at  $p_c \approx 2000$  Atm. It is remarkable that the extended Wendt-Abraham parameter  $r_{\alpha,\beta}^{WA}$  is more sensitive to detect these structural transformations than other parameters,  $S_2^{\alpha,\beta}$  and  $\rho_{\alpha,\beta}$ . This can be considered directly as an evidence that the structural transformations detected at  $p_c \approx 2000$  Atm are related with the changes of the local, short-range order, since the parameter  $r_{\alpha,\beta}^{WA}$  probes the structural properties inside of the first coordination shell whereas the quantities  $S_2^{\alpha,\beta}$  and  $\rho_{\alpha,\beta}$  characterize features at more extended spatial scales.

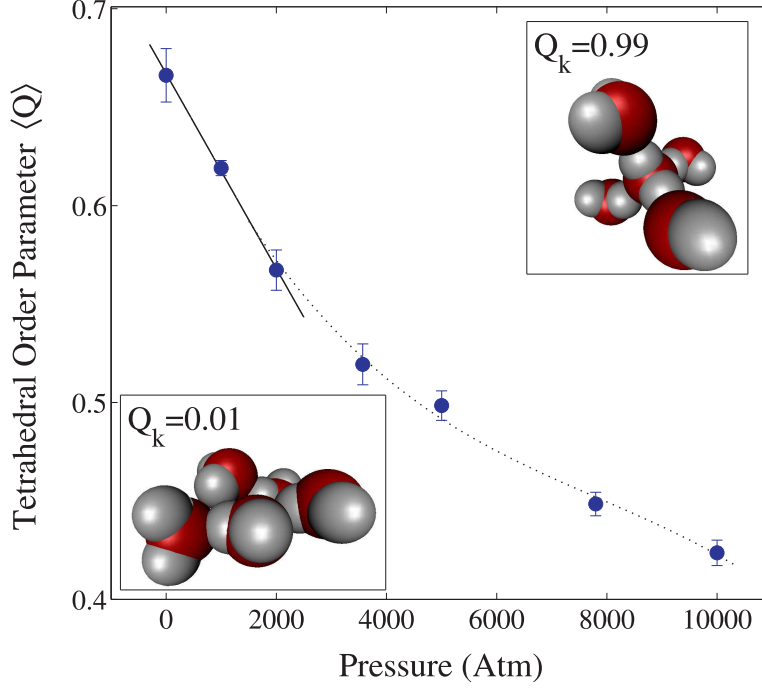


Fig. 5. (color online) Main: Tetrahedral order parameter *versus* pressure at the temperature  $T = 277$  K. Inset: Instantaneous configurations of water molecules at the two values of the tetrahedral order parameter:  $Q_k = 0.01$  (the four bonds are practically aligned) and  $Q_k = 0.99$  (molecular system is close to be a perfect tetrahedron).

### 3.4 Tetrahedral Order Parameter

The tetrahedral order parameter  $Q_k$  can be used to quantify the tetrahedrality within the first shell [28]. This parameter is defined as

$$Q_k = 1 - \frac{3}{8} \sum_{i=1}^3 \sum_{j=i+1}^4 \left[ \cos \theta_{ikj} + \frac{1}{3} \right]^2. \quad (9)$$

The term  $\theta_{ikj}$  is the angle formed between the central molecule  $k$  and its neighbors  $i$  and  $j$ . The average value

$$\langle Q \rangle = \frac{1}{N} \sum_{k=1}^N Q_k \quad (10)$$

quantifies directly the orientational order within the first shell. For the perfect tetrahedral order, one has  $\langle Q \rangle = 1$ ; if the bonds are arranged in a manner with the absence of tetrahedral geometry, one has  $\langle Q \rangle = 0$ . So, with the deviation from the perfect tetrahedron the values of  $\langle Q \rangle$  demonstrate decrease.

The pressure dependence of the tetrahedral order parameter  $\langle Q \rangle$  for liquid water at the temperature  $T = 277$  K is presented in Fig. 5. As can be seen, with the increase of the applied pressure the tetrahedral order parameter demonstrates a nonlinear decrease. Such a behavior of the parameter indicates on the decrease of the amount of tetrahedral structures in liquid water with the isothermal increase of the pressure  $p$ , that is in agreement with the results of Ref. [27]. It is necessary to note that although the behavior of the tetrahedral order parameter  $\langle Q \rangle$  changes with the pressure  $p$ , this parameter  $\langle Q \rangle$  demonstrates no a sharp transition from low-density phase to high-density one.

### 3.5 Dynamic Structure Factor and Dispersion of Sound Velocity

According to a definition (see Ref. [43]), the dynamic structure factor  $S(k, \omega)$  is related with the Fourier transform of the intermediate scattering function  $F(k, t)$

$$S(k, \omega) = \frac{1}{\pi} \int_0^{\infty} F(k, t) \cos(\omega t) dt. \quad (11)$$

Here

$$F(k, t) = \frac{1}{N} \left\langle \sum_l e^{i\mathbf{k} \cdot \mathbf{r}_l(0)} \sum_j e^{-i\mathbf{k} \cdot \mathbf{r}_j(t)} \right\rangle = \langle \delta\rho_k(0) \delta\rho_k^*(t) \rangle, \quad (12)$$

where  $\delta\rho_k(t)$  is the  $k$ -component of the fluctuation of the microscopic number density  $\rho_k(t)$ . Nevertheless, because of the long-time tails of  $F(k, t)$  in water (see Ref. [51]), the finding of the dynamic structure factor spectra  $S(k, \omega)$  by means of Eqs. (11) and (12) yields the significant inaccuracies. To avoid this problem we use the Wiener-Khinchin (statistical-autocorrelation) theorem [52], which allows one to rewrite Eq. (11) in the next identical form

$$S(k, \omega) = \frac{1}{t_M} \left| \int_0^{t_M} \delta\rho_k(t) e^{i\omega t} dt \right|^2, \quad (13)$$

where  $t_M$  is the observation time for the variable  $\delta\rho_k(t)$ . Eq. (13) gives a possibility to find  $S(k, \omega)$  from the dynamical variable  $\delta\rho_k(t)$ , directly. Note that an advantage of Eq. (13) over Eq. (11) is related with the saving of computational time, that is very important at numerical estimations. Then, the dynamic structure factor  $S(k, \omega)$  can be evaluated at these  $k$ -values, which are allowed by the system size:  $k = 2\pi/L(n, m, l)$ , where  $n, m, l$  are integers.

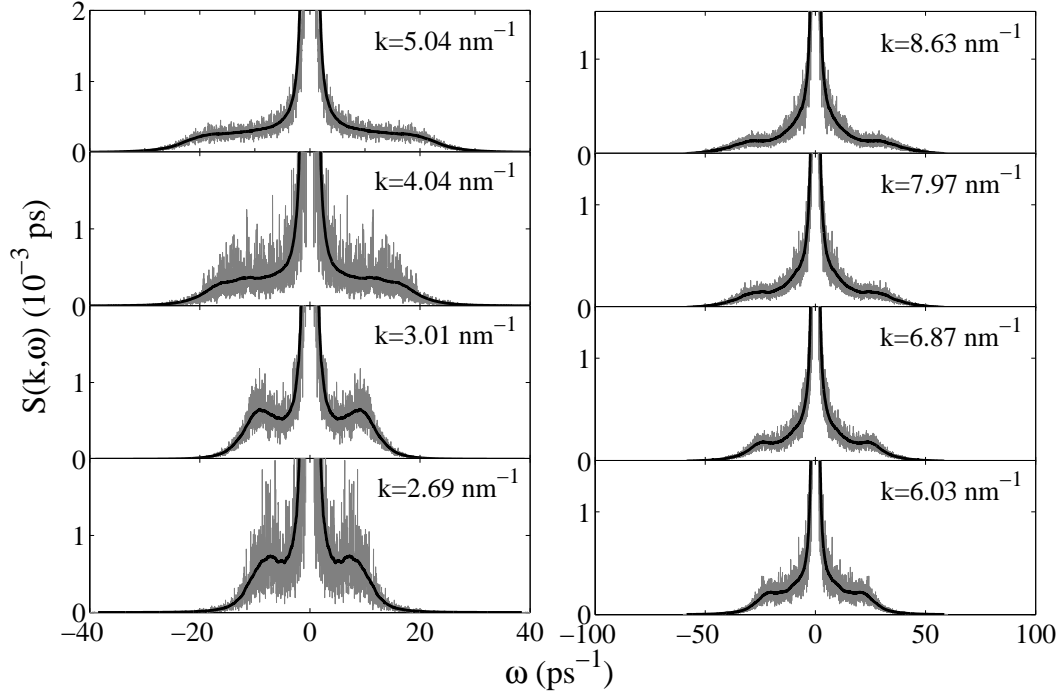


Fig. 6. (color online) Dynamic structure factor of liquid water at the temperature  $T = 277$  K and the pressure  $p = 3750$  Atm for different values of the wave number  $k$ : the noisy (gray) lines represent the results obtained from molecular dynamics simulation data and Eq. (13), thick (black) lines are results of the smoothing procedure.

The size of our system allows one to take the smallest value of  $k \approx 1.38 \text{ nm}^{-1}$ . To delete the noises from dynamic structure factor spectra  $S(k, \omega)$  we apply the smoothing procedure based on the computation of the arithmetic mean for the local window with the length  $1.0 \text{ ps}^{-1}$ .

The frequency spectra of the dynamic structure factor  $S(k, \omega)$  of water for different values of the wave number  $k = 2.69 \div 8.63 \text{ nm}^{-1}$  at the temperature  $T = 277$  K and the pressure  $p = 3750$  Atm (that is higher than  $p_c$ ) are presented in Fig. 6. Here, the high frequency collective excitations responsible for sound propagation in the system are clearly detected for all the considered values of  $k$ . To obtain the precise values of the sound velocity  $\omega_c(k)$  which is related with the high-frequency peak-position in  $S(k, \omega)$ , we consider the longitudinal current spectra  $C_L(k, \omega)$  [53]. This term can be found from the dynamic structure factor  $S(k, \omega)$  by the way:

$$C_L(k, \omega) = \frac{\omega^2}{k^2} S(k, \omega). \quad (14)$$

On Fig. 7, the dispersion of sound velocity  $\omega_c(k)$  in water at the temperatures  $T = 277$  K and  $T = 297$  K and the pressures  $p = 3750$  Atm and  $p = 7797$  Atm are presented. Results of molecular dynamics simulations with the

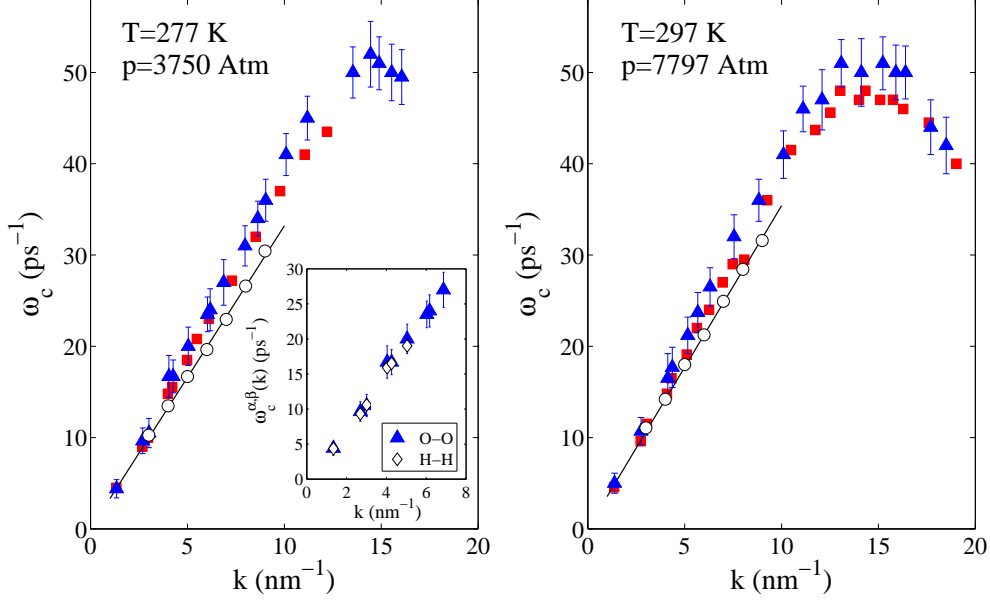


Fig. 7. (color online) Main: Dispersion of sound velocity  $\omega_c(k)$ : circles represent the experimental data [54]; triangles are results of molecular dynamics simulations data with Amoeba potential; squares represent results of computer simulations with TIP5P potential; solid line indicates the best linear fit to experimental data, and the slope corresponds to the sound velocity  $\vartheta = 3320 \text{ m/s}$  ( $\vartheta = 3540 \text{ m/s}$ ) at the temperature  $T = 277 \text{ K}$  ( $T = 297 \text{ K}$ ). Inset: Partial dispersion of sound velocity  $\omega_c^{\alpha,\beta}(k)$ .

Amoeba model potential reproduce correctly the experimental inelastic X-ray scattering data [54]. Moreover, with the increase of  $k$  the simulations results overestimate slightly the experimental data for sound velocity of Ref. [54]. The comparison of the results with the two potentials reveals that data obtained on the basis TIP5P are in the range of inaccuracies of the dispersion curve obtained on the basis Amoeba potential and have a better agreement with experimental data. Nevertheless, simulation data with TIP5P demonstrate also overestimated values in comparison with the experimental outcomes of inelastic X-ray scattering.

The partial dispersion of sound velocity  $\omega_c^{\alpha,\beta}(k)$  for  $O$  and  $H$  atoms obtained with the Amoeba potential is given in inset of Fig. 7. As can be seen, both lines are identical. This is direct evidence that the main influence on the features of sound propagation in water appear due to oxygen, which is the heavy component of a water molecule. Note that this is agreed with results of Ref. [55] (p. 7235).

To estimate quantitatively the pressure dependence on the properties of the collective dynamics in water we show in Fig. 8 the density and pressure dependence of the sound velocity  $\vartheta$ , where results of our molecular dynamics simulations data are compared with experimental data [54]. First, as can be seen

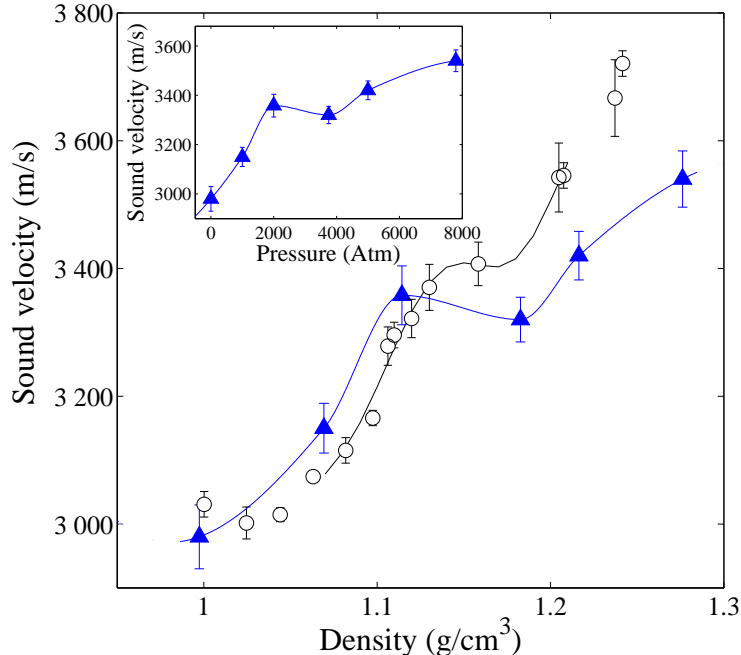


Fig. 8. (color online) Main: Density dependence of the sound velocity  $\vartheta$ : the circles represent the experimental IXS data [54], the triangles are results of our molecular dynamics simulations with Amoeba water model. Solid line is the spline-interpolation. Inset: Pressure dependence of the sound velocity obtained from simulations.

from figure, results of the molecular dynamics simulations reproduce correctly the experimental data for sound velocity [54]. An insignificant understatement of  $\vartheta$  appears from simulations in comparison with experimental data at high densities. Nevertheless, both our numerical results and experimental inelastic X-ray scattering data reveal clearly a changes in dynamics at the density  $\rho_c = 1.114 \div 1.12 \text{ g/cm}^3$ . Note that such density of the investigated water system corresponds to the pressure  $p_c \approx 2000 \text{ Atm}$  (see inset of Fig. 8), at which the structural transformations were detected by the order characteristics.

Thus, the structural and dynamic anomalies observed in water at the pressure  $p_c \approx 2000 \text{ Atm}$  are provided by the local structural molecular rearrangement inside of the first two coordination shells. It is necessary to note that such a treatment is also suggested by results of Ref. [32], where anomalies in water were studied on the basis of the five-site transferable interaction potential (TIP5P). It was found in Ref. [32] that the anomalous decrease of orientational order upon compression occurs in the first and second coordination shells, but the anomalous decrease of translational order upon compression occurs mainly in the second shell.

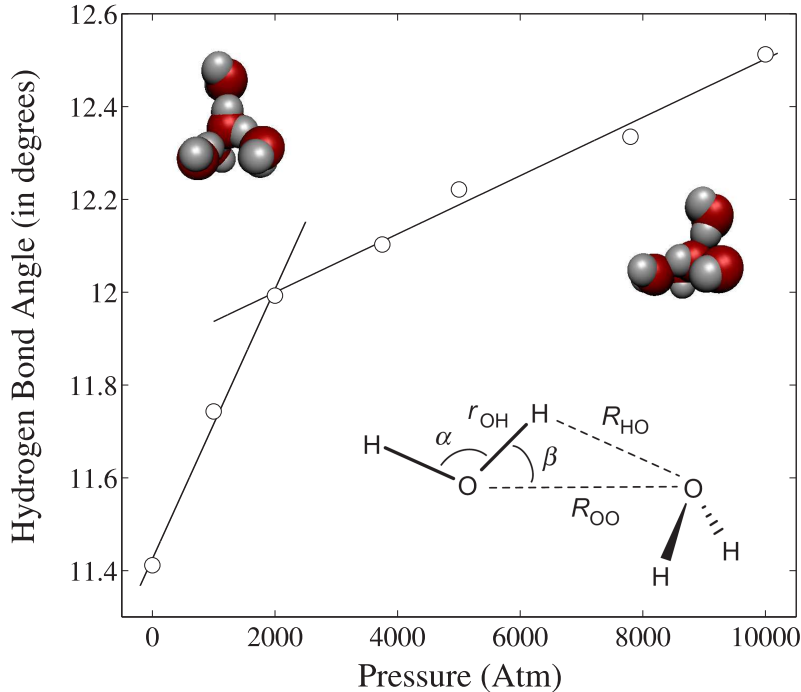


Fig. 9. (color online) Pressure dependence of the hydrogen bond angle.

### 3.6 Hydrogen-Bond Network

A detailed description of the hydrogen-bond network in liquid water is the key to understanding its unusual properties. The studies of the hydrogen-bonded network structure in water have mainly relied on neutron and X-ray diffraction, infrared spectroscopies, and computer simulations techniques [56]. Experimental data from noncrystalline materials provide the radial distribution functions and static structure factors [48] that do not provide angular correlations needed to assign uniquely the local geometries in water [57]. In order to understand the effect of the structure on the dynamics we carried out a detailed analysis of the pressure dependence of the hydrogen bond angle [58,59]. In the same lines with the work [60], we use a *geometric criterion*. According to this criterion two water molecules are taken to be hydrogen-bonded if their inter-oxygen distance is less than  $3.5 \text{ \AA}$  and simultaneously the oxygen-hydrogen distance is less than  $2.45 \text{ \AA}$  and the oxygen-oxygen-hydrogen angle  $\beta$  is less than  $30^\circ$ . We note that the critical distances of  $3.5 \text{ \AA}$  and  $2.45 \text{ \AA}$  are essentially the positions of the first minimum in the oxygen-oxygen and oxygen-hydrogen radial distribution functions, respectively. All the terms of this algorithm are presented in the bottom inset of Fig. 9. The behavior of the hydrogen bond angle  $\beta$  at the temperature  $T = 277 \text{ K}$  is illustrated in Fig. 9. This quantity is presented as an averaged over all possible hydrogen-bond environments. As can be seen from the figure, the distinct changes in the behavior of the angle  $\beta$  at critical pressure  $p = 2000 \text{ atm}$  is observed.

In the inset of Fig. 9, we show the configurations of water molecules at the applied pressure  $p = 1.0$  Atm (on the left of Fig. 9) and  $p = 10000$  Atm (on the right of Fig. 9) in the neighborhood of four closest molecules, which are connected by hydrogen bonds. Thereby, we confirm quantitatively the idea that the structural and dynamical anomalies of water are related with the local structural rearrangement of molecules within first two coordination shells [32], which specifies by deformation of the hydrogen-bond network.

## 4 Conclusions

Molecular dynamics simulations of liquid water at the temperature  $T = 277$  K and the range of pressure  $p = 1.0 \div 10\,000$  Atm are performed on the basis of model Amoeba potential [36]. It is found that this potential reproduces correctly equilibrium structural and dynamical properties of liquid water, although TIP5P potential yields a better agreement with experimental data.

The pressure dependence of the structural characteristics and order parameters detects clearly the appearance of the structural anomaly [32] in the water system at the temperature  $T = 277$  K and the pressure  $p \approx 2000$  Atm. The detailed analysis of the extended Wendt-Abraham parameter, pair-correlation entropy and translational order parameter indicates that the observed structural transformations occur in the hydrogen/oxygen atoms in the range of the first two coordination shells. Thus, these structural transformations are correlated with the deformation of the hydrogen-bond network [59]. Moreover, it is found that with the increase of the applied pressure, a fraction of tetrahedral structures in the system decreases. The tetrahedral order parameter  $\langle Q \rangle$  demonstrates no a sharp transition from low-density state to high-density one.

We have found that the structural anomaly has an impact on the dynamic properties of the liquid water. The computed spectra of the dynamic structure factor  $S(k, \omega)$  at high pressures reveal all features (including the high-frequency acoustic mode) typical for liquid systems [4,61,62]. The found sound dispersions are in a good agreement with the experimental inelastic X-ray scattering data [54]. It is found the main features of sound propagation in liquid water are related with the oxygen atom.

The pressure dependence of the sound velocity indicates on the anomalous dynamics in water at the same value of the pressure as for the structural anomaly,  $p \approx 2000$  Atm (the temperature  $T = 277$  K), that corresponds to the density  $\rho_c \approx 1.12$  g/cm<sup>3</sup>.

## 5 Acknowledgments

We dedicate this paper to the memory of Professor Renat M. Yulmetyev. This work was supported by the grants of Russian Foundation for Basic Research (No. 08-02-00123-a and No. 09-02-91053-CNRS-a).

## References

- [1] *Water: A Comprehensive Treatise*, edited by F. Franks (Plenum, New York, 1972), Vol. 1.
- [2] F.H. Stillinger, *Science* 209 (1980) 451.
- [3] D. Eisenberg and V. Kauzmann, *The Structure and Properties of Water*, Clarendon Press, Oxford (2005).
- [4] A.V. Mokshin, R.M. Yulmetyev and P. Hänggi, *Phys. Rev. Lett.* 95 (2005) 200601.
- [5] A. Geiger, F.H. Stillinger, A. Rahman, *J. Chem. Phys.* 70 (1979) 4185.
- [6] H.E. Stanley, J. Teixeira, *J. Chem. Phys.* 73 (1980) 3404.
- [7] J.A. Barker and R.O. Watts, *Chem. Phys. Lett.* 3 (1969) 144.
- [8] J.S. Rowlinson, *Trans. Faraday Soc.* 47 (1951) 120.
- [9] A. Rahman, F.H. Stillinger, *J. Chem. Phys.* 55 (1971) 3336.
- [10] P.H. Poole, F. Sciortino, U. Essmann and H.E. Stanley, *Nature* 360 (1992) 324.
- [11] B. Guillot, *J. Mol. Liq.* 101 (2002) 219.
- [12] J.D. Bernal, R.H. Fowler, *J. Chem. Phys.* 1 (1933) 515.
- [13] L. Laasonen, F. Csajka and M. Parrinello, *Chem. Phys. Lett.* 194 (1992) 172.
- [14] M. Bernasconi, P. L. Silvestrelli, and M. Parrinello, *Phys. Rev. Lett.* 81 (1998) 1235.
- [15] P.L. Silvestrelli and M. Parrinello, *Phys. Rev. Lett.* 82 (1999) 3308.
- [16] E. Schwegler, G. Galli, and F. Gygi, *Phys. Rev. Lett.* 84 (2000) 2429.
- [17] M. Boero, K. Terakura, T. Ikeshoji, C.C. Liew, and M. Parrinello, *J. Chem. Phys.* 115 (2001) 2219.
- [18] I.-F.W. Kuo, Ch. J. Mundy, M.J. McGrath et al, *J. Phys. Chem. B* 108 (2004) 12998.
- [19] D. Lu, F. Gygi and G. Galli, *Phys. Rev. Lett.* 100 (2008) 147601.

- [20] Y. Katayama, T. Hattori, H. Saitoh, T. Ikeda, and K. Aoki, Phys. Rev. B 81 (2010) 014109.
- [21] Sh.H. Khan, G. Matei, Sh. Patil, and P.M. Hoffmann, Phys. Rev. Lett. 105 (2010) 106101.
- [22] S. Han, M. Y. Choi, P. Kumar, and H. E. Stanley, Nature Physics 6 (2010) 685.
- [23] P. Gallo, M. Rovere and S.-H. Chen, J. Phys. Chem. Lett. 1 ( 2010) 729.
- [24] E. Schwegler, G. Galli, F. Gygi, R.Q. Hood, Phys. Rev. Lett. 87 (2001) 265501.
- [25] E. Sanz, C. Vega, J.L.F. Abascal, and L.G. MacDowell, Phys. Rev. Lett. 92 (2004) 255701.
- [26] P.A. Netz, F.W. Starr, M.C. Barbosa, H.E. Stanley, Physica A 314 (2002) 470.
- [27] A.K. Soper, M.A. Ricci, Phys. Rev. Lett. 84 (2000) 2881.
- [28] J.R. Errington and P.G. Debenedetti, Nature (London) 409 (2001) 318.
- [29] A.M. Saitta and F. Datchi, Phys. Rev. E 67 (2003) 020201(R).
- [30] F. Li, Q. Cui, Zh. He, T. Cui, J. Zhang, Q. Zhou, G. Zou, and Sh. Sasaki, J. Chem. Phys. 123 (2005) 174511.
- [31] R. Esposito, F. Saija, A.M. Saitta, and P.V. Giaquinta, Phys. Rev. E 73 (2006) 040502(R).
- [32] Zh. Yan, S.V. Buldyrev, P. Kumar, N. Giovambattista, P.G. Debenedetti, H.E. Stanley, Phys. Rev. E 76 (2007) 051201.
- [33] W.P. Krekelberg, J. Mittal, V. Ganesan, and Th.M. Truskett, J. Chem. Phys. 127 (2007) 044502.
- [34] W.P. Krekelberg, J. Mittal, V. Ganesan and Th.M. Truskett, Phys. Rev. E 77 (2008) 041201.
- [35] P.G. Debenedetti, J. Phys.: Cond. Matt. 15 (2003) R1669.
- [36] J.W. Ponder, *TINKER: Software Tools for Molecular Design*; 4.1 ed.: Washington University School of Medicine: Saint Louis, 2003.
- [37] P. Ren and J.W. Ponder, J. Phys. Chem. B 107 (2003) 5933.
- [38] P. Ren and J.W. Ponder, J. Phys. Chem. B 108 (2004) 13427.
- [39] M.P. Allen and D.J. Tildesley, *Computer Simulation of Liquids*, Clarendon Press, Oxford (1987).
- [40] H.J.C. Berendsen, J.P.M. Postma, W.F. van Gunsteren, A. DiNola, J.R. Haak, J. Chem. Phys. 81 (1984) 3684.
- [41] A.K. Soper, M.G. Philips, J. Chem. Phys. 107 (1986) 47.

- [42] G. Hura, J.M. Sorenson, R.M. Glaeser, T. Head-Gordon, J. Chem. Phys. 113 (2000) 9140.
- [43] J.P. Hansen and I.R. McDonald, *Theory of Simple Liquids*, Academic Press, New York (2006).
- [44] A.D. Becke, J. Chem. Phys. 98 (1993) 5648.
- [45] C. Lee, W. Yang, R.G. Parr, Phys. Rev. B 37 (1988) 785.
- [46] <http://www.pwscf.org>.
- [47] *Ab-initio* molecular dynamics was performed within the DFT framework, employing a plane-wave formalism together with the BLYP (Becke-Lee-Yang-Parr) exchange-correlation functional and norm-conserving pseudopotentials [44,45] on the basis of the Quantum-Espresso code [46]. The temperature was controlled by a single Nose-Hoover thermostat on the ions (the electronic thermostat is not applied in our simulations).
- [48] A.K. Soper, Chem. Phys. 258 (2000) 121.
- [49] H.R. Wendt and F.F. Abraham, Phys. Rev. Lett. 41 (1978) 1244.
- [50] H. Tanaka, Phys. Rev. Lett. 80 (1998) 5750.
- [51] E. Harder, J.D. Eaves, A. Tokmakoff, and B.J. Berne, PNAS 102 (2005) 11611.
- [52] G.A. Korn and T.M. Korn, *Mathematical Handbook for Scientists and Engineers*, McGraw-Hill Book Co., New York (1961).
- [53] G. Ruocco and F. Sette, J. Phys.: Condens. Matter 11 (1999) R259.
- [54] M. Krisch, P. Loubeyre, G. Ruocco et al, Phys. Rev. Lett. 89 (2002) 125502.
- [55] M.A. Ricci, D. Rocca, G. Ruocco, R. Vallauri, Phys. Rev. A 40 (1989) 7226.
- [56] R. Ludwig, Angew. Chem. Int. Ed. Engl. 40 (2001) 1808.
- [57] P.G. Kusalik, I.M. Svishchev, Science 265 (1994) 1219.
- [58] M.F. Chaplin, *Water Structure Science*, (2007). <http://www1.lsbu.ac.uk/water/hbond.html>.
- [59] K. Modig, B.G. Pfrommer and B. Halle, Phys. Rev. Lett. 90 (2003) 075502.
- [60] A. Luzar, D. Chandler, J. Chem. Phys. 98 (1993) 8160.
- [61] R.M. Yulmetyev, A.V. Mokshin, P. Hänggi and V. Yu. Shurygin, Phys. Rev. E 64 (2001) 057101.
- [62] T. Scopigno, G. Ruocco and F. Sette, Rev. Mod. Phys. 77 (2005) 881.